THE JOURNAL OF BIOLOGICAL CHEMISTRY VOL. 286, NO. 34, pp. 29797–29805, August 26, 2011

Fibrinogen Is a Ligand for the *Staphylococcus aureus* Microbial Surface Components Recognizing Adhesive Matrix Molecules (MSCRAMM) Bone Sialoprotein-binding Protein (Bbp)

Received for publication, December 21, 2010, and in revised form, May 6, 2011 Published, JBC Papers in Press, June 3, 2011, DOI 10.1074/jbc.M110.214981

Vanessa Vazquez[‡§], Xiaowen Liang[‡], Jenny K. Horndahl[‡], Vannakambadi K. Ganesh[‡], Emanuel Smeds[‡], Timothy J. Foster[¶1], and Magnus Hook[‡2]

From the [‡]Center for Infectious and Inflammatory Diseases, Institute of Biosciences and Technology, Texas A&M University System Health Science Center, Houston, Texas 77030, the [§]Graduate School of Biomedical Sciences, University of Texas Health Science Center, Houston, Texas 77030, and the [¶]Moyne Institute of Preventive Medicine, Department of Microbiology, Trinity College, Dublin 2, Ireland

Microbial surface components recognizing adhesive matrix molecules (MSCRAMMs) are bacterial surface proteins mediating adherence of the microbes to components of the extracellular matrix of the host. On Staphylococci, the MSCRAMMs often have multiple ligands. Consequently, we hypothesized that the *Staphylococcus aureus* MSCRAMM bone sialoprotein-binding protein (Bbp) might recognize host molecules other than the identified bone protein. A ligand screen revealed that Bbp binds human fibrinogen (Fg) but not Fg from other mammals. We have characterized the interaction between Bbp and Fg. The binding site for Bbp was mapped to residues 561–575 in the Fg Aα chain using recombinant Fg chains and truncation mutants in Far Western blots and solid-phase binding assays. Surface plasmon resonance was used to determine the affinity of Bbp for Fg. The interaction of Bbp with Fg peptides corresponding to the mapped residues was further characterized using isothermal titration calorimetry. In addition, Bbp expressed on the surface of bacteria mediated adherence to immobilized Fg Aα. Also, Bbp interferes with thrombin-induced Fg coagulation. Together these data demonstrate that human Fg is a ligand for Bbp and that Bbp can manipulate the biology of the Fg ligand in the host.

Staphylococcus aureus uses secreted and cell surface-associated virulence factors to cause disease ranging from mild skin infections such as folliculitis and impetigo to life-threatening illnesses such as sepsis and pneumonia (1). Microbial surface components recognizing adhesive matrix molecules (MSCRAMMs)[3] are surface proteins used by bacteria to interact with host molecules such as collagen, fibronectin, and fibrinogen (Fg). The Sdr proteins are a subset of putative staphylococcal MSCRAMMs, covalently anchored to the cell wall and characterized by a segment composed of repeated serine-aspartate (SD) dipeptides. The Sdr proteins have similar structural organization where the N-terminal ligand-binding A region can be further divided into three subdomains (N1, N2, and N3), where N2 and N3 adopt IgG-like folds. The A-region is often followed by a B region that consists of repeated β-sandwich domains. The carboxyl-terminal section of the proteins contains the serine-aspartate repeats followed by motifs required for cell wall anchoring (2).

A dynamic ligand binding mechanism called the "dock, lock, and latch" was revealed by biochemical and structural studies of the fibrinogen-binding *Staphylococcus epidermidis* MSCRAMM SdrG (3). SdrG binds to a linear sequence in the N terminus of the Bβ chain of human Fg. The SdrG-binding sequence includes the thrombin cleavage site, and the MSCRAMM inhibits thrombin-catalyzed release of fibrinopeptide B and fibrin formation (3, 4). Binding is initiated by the "docking" of the ligand peptide into the trench formed between the N2 and N3 IgG domains. Next, the ligand is "locked" in place by interactions with residues at the extension of the C terminus of N3 that are redirected to cover the bound ligand peptide. Following the "lock" event, the "latch" region in the N3 extension stabilizes the ligand-MSCRAMM complex by inserting into the N2 domain through a β-strand complementation (3, 5). Because the Sdr proteins are similar in domain organization and folding, the dock, lock, and latch mechanism has been proposed as a general mechanism of ligand binding for this subfamily of MSCRAMMs.

Fibrinogen is a large dimeric protein composed of three polypeptides, Aα, Bβ, and γ, with key roles in blood coagulation, thrombosis, and host defense (6–8). Known Fg-binding MSCRAMMS on *S. aureus* include the clumping factors (ClfA and ClfB) and the fibronectin-binding proteins (FnbpA and FnbpB) (9–12). ClfB binds to a site in the central part of the Aα chain C terminus, whereas ClfA and the Fnbps bind to the extreme C terminus of the Fg γ chain (11, 13, 14). Each of these Fg-binding MSCRAMMs interacts with additional ligands. ClfA binds to complement factor I (15), and ClfB binds to

[1] Supported by Science Foundation Ireland.
[2] Supported by Grant AI 20624 from the National Institutes of Health. To whom correspondence should be addressed: Center for Infectious and Inflammatory Diseases, Texas A&M University System Health Science Center, Institute of Biosciences and Technology, 2121 West Holcombe Blvd., Ste. 603, Houston, TX 77030. Tel.: 713-677-7551; Fax: 713-677-7576; E-mail: mhook@ibt.tamhsc.edu.
[3] The abbreviations used are: MSCRAMM, microbial surface components recognizing adhesive matrix molecules; Bbp, bone sialoprotein-binding protein; Fg, fibrinogen; Clf, clumping factor; Fnbp, fibronectin-binding protein; MRSA, methicillin-resistant *S. aureus*; SPR, surface plasmon resonance; ITC, isothermal titration calorimetry; Sdr, SD repeat.

cytokeratin 10 (16). FnbpA binds to elastin, and both FnbpA and FnbpB bind to fibronectin (11).

We hypothesized that Bbp might also recognize multiple host proteins. A ligand screen revealed that Bbp_{N2N3} recognizes human Fg, and the initial characterization of this interaction is reported here.

EXPERIMENTAL PROCEDURES

Media and Growth Conditions—*Escherichia coli* strains were cultured at 37 °C with shaking in Luria broth (Sigma) supplemented with ampicillin (100 μg/ml). *Lactococcus lactis* was cultured in M17 (Oxoid) supplemented with glucose (0.5%) and erythromycin (5 μg/ml) at 30 °C overnight. *S. aureus* MRSA252 was cultured in brain heart infusion broth (Remel) at 37 °C with shaking. *S. aureus* Newman derivatives were cultured in brain heart infusion broth supplemented with erythromycin (5 μg/ml), tetracycline (2 μg/ml), and/or chloramphenicol (10 μg/ml) as needed to exponential phase.

Recombinant Proteins—A recombinant Bbp construct corresponding to the (N2N3 domains) amino acids 270–599 of previously published sequences was engineered (17). The amplification primer sequences are listed in Table 1. All oligonucleotides used for this study were purchased from Integrated DNA Technologies. *E. coli* expressing full-length recombinant His-tagged Fg chains Aα, Bβ, and γ have been previously described (18–20). A plasmid encoding the Fg Aα sequence was used as template to amplify the DNA encoding truncated Aα protein corresponding to residues 1–575 and 1–560 (Table 2). Selected plasmids were digested, and the inserts were ligated to pQE30 and transformed into XL-1 Blue cells followed by sequence verification of plasmids pQE30-Bbp_{N2N3}, pQE30-Aα1–575, and pQE30-Aα1–560. Recombinant protein expression was induced with isopropyl-1-thio-β-D-galactopyranoside (Gold Biotechnology), and expressed protein was purified by Ni^{2+} affinity chromatography on a HiTrap chelating column (GE Healthcare) followed by anion-exchange chromatography using a Q HP Sepharose column (GE Healthcare), as described previously (4). The His-tagged recombinant Fg chains, Aα, Aα1–560, Aα1–575, Bβ, and γ were recovered from inclusion bodies, and purification was performed in the presence of 8 M urea (Sigma). To assess protein purity, pooled fractions were separated on 10% SDS-PAGE and stained with Coomassie Blue or electrotransferred to nitrocellulose for Western blotting with anti-His monoclonal antibody (GE Healthcare) followed by anti-mouse-AP (Bio-Rad). The mass of Bbp_{N2N3} was determined to be 37,491.4 Daltons (not shown) by mass spectrometry, which is similar to the predicted mass of 37,837.6 Daltons.

Rabbit-anti-Bbp_{N2N3} Antibodies—Rabbit polyclonal antiserum to Bbp_{N2N3} was generated at Rockland Immunochemicals using the fast protocol. IgG was purified using protein A-Sepharose (Thermo Fisher) affinity chromatography. Next, the IgG was cleared for cross-reactive binding to other Sdr proteins before positive affinity purification on Bbp_{N2N3} coupled to EZ-Link beads (Thermo Fisher). This preparation, followed by goat-anti-rabbit HRP, was used to detect Bbp_{N2N3} binding in solid-phase assays.

Homology Modeling—The predicted ligand-binding subdomains of Bbp_{N2N3} were modeled based on the previously determined crystal structure of SdrG (Protein Data Bank ID 1RI7) (3). The $SdrG_{N2N3}$ and Bbp_{N2N3} share ~50% sequence identity. The homology modeling was performed using the Homology module in the InsightII software (Acclrys Inc.). The ribbon figure was made with RIBBONS software (21).

Solid-phase Binding Assays—To conduct a Bbp_{N2N3} ligand screen with extracellular matrix and plasma proteins, 1 μg of human fibrinogen depleted of plasminogen and von Willebrand factor (Enzyme Research), human fibronectin (Chemicon), BSA, collagen type I from rat tail tendons (Cultrex R&D), bovine nasal septum type II collagen (Sigma), recombinant human collagen type III (FibroGen), fibroblast and epithelial cell co-culture collagen type IV (Sigma), and bovine neck ligament elastin (Sigma) or 10 μg of murine sarcoma basement membrane laminin (Sigma) were coated on microtiter wells overnight. The wells were washed, blocked, and incubated with 100 μl of Bbp_{N2N3} (0.1–10 μM) and developed with anti-His tag antibodies.

To detect binding of immobilized Bbp to soluble Fg, microtiter wells were coated with increasing amounts of Bbp_{N2N3} (0.25–2.5 μg). The wells were washed, blocked, probed with

TABLE 1
Oligonucleotides used in this study
Restriction sites are underlined.

Primer name	Oligonucleotide sequence
pQE30-BbpF	CCCGGATCCGTTGCTTCAAACAATGTTAATGAT
pQE30-BbpR	CCCAAGCTTTTATTCAGGTTTAACAGTACCGTCACC
pQE30-FgAα1F	CGGGATCCGCAGATAGTGGTGAAGGT
pQE30-FgAα1–575R	CGAAGCTTTTAGGAGTCTCCTCTGTTGTAACT
pQE30-FgAα1–560R	CGAAGCTTTTAGTAACTTGAAGATTTACCACG
pCU1-BbpPrF	CGGGATCCGATATAACATACATCAACAT
pCU1-BbpTrR	CGTCTAGAATATTATCGCCTCATATAAG

TABLE 2
Constructs used in this study

Construct	Vector	Residues	Source
E. coli Bbp_{N2N3}	pQE30	270–599	This study
E. coli $SdrG_{N2N3}$	pQE30	273–597	(3)
E. coli $ClfA_{N2N3}$	pQE30	229–545	(27)
E. coli Fg Aα	pQE30	Full-length mature Aα	(18)
E. coli Fg Aα1–575	pQE30	1–575 of mature Aα	This study
E. coli Fg Aα1–560	pQE30	1–560 of mature Aα	This study
E. coli Fg Bβ	pQE30	Full-length mature Bβ	(19)
E. coli Fg γ	pQE30	Full-length mature γ	(20)
L. lactis-vector	pKS80	Empty vector	(23)
L. lactis-Bbp	pKS80	Full-length Bbp	This study
S. aureus Newman DU6023-pCU1	pCU1	Empty vector	(23)
S. aureus Newman DU6023-pCU1-Bbp	pCU1	Full-length Bbp (with promoter and terminator)	This study

TABLE 3
Peptides synthesized for this study

Peptide name	Peptide sequence
Fg Aα551–575	FPSRGKSSSYSKQFTSSTSYNRGDS
Fg Aα551–565	FPSRGKSSSYSKQFT
Fg Aα556–570	KSSSYSKQFTSSTSY
Fg Aα561–575	SKQFTSSTSYNRGDS
Fg AαScr	TSSTRGDSSYNSKQF
Fg AαCanine	SKQFVTSSTTYNRGDS

100 μl of soluble Fg (1 μM), and developed with goat-anti-human fibrinogen (Sigma) followed by donkey-anti-goat-HRP (Applied Biological Materials).

To determine binding of MSCRAMMs to Fg, microtiter wells were coated with 1 μg of human, mouse (Enzyme Research), cat, dog, cow, sheep, and pig (Sigma) fibrinogen or recombinant human Fg polypeptides. The wells were subsequently washed, blocked, and probed with 100 μl of Bbp_{N2N3} or $ClfA_{N2N3}$ at the indicated concentrations followed by protein-specific rabbit antibodies and goat-anti-rabbit HRP (Bio-Rad).

In peptide inhibition experiments, 150 nM Bbp_{N2N3} was incubated with increasing concentrations (0.1–30 μM) of Fg Aα peptides synthesized by Biomatik (Table 3) for 30 min before 100 μl of the mixture was transferred to Fg-coated wells. MSCRAMM binding was detected as described above.

All proteins were coated at 4 °C in bicarbonate buffer, pH 8.3. All wells were washed with Tris-buffered saline containing 0.1% Tween 20, blocked with Superblock (Thermo Fisher), and developed with SigmaFast OPD, and the absorbance at 450 nm was measured using a Thermo Max plate reader and plotted with GraphPad Prism 4.

Surface Plasmon Resonance (SPR)—SPR analysis was performed at 25 °C on a BIAcore 3000 system using a CM5 chip (GE Healthcare). The ligand surface was prepared via amine coupling. Fg (12 μl of 10 μg/ml in sodium acetate, pH 5.5) was injected over an activated flow cell at 5 μl/min for 3 min using HEPES-buffered saline containing 0.005% Tween 20 as the running buffer. Approximately 1600 response units of human Fg were immobilized. A second uncoupled flow cell was activated and deactivated to serve as a reference cell. Increasing concentrations of Bbp_{N2N3} (40 nM–2.56 μM in TBS, 0.005% Tween 20) were injected at 30 μl/min over ligand and reference surfaces. After subtraction of reference cell from the experimental cell sensorgrams, the baseline-corrected SPR response curves were globally fitted to the 1:1 (Langmuir) binding model using the BIAevaluation software. Association and dissociation rate constants (k_a, k_d) were obtained from the fitting, and a dissociation constant (K_D) was calculated ($K_D = k_d/k_a$). Responses at equilibrium of the SPR curves were fitted to a one-site binding isotherm (GraphPad Prism 4) to obtain the equilibrium K_D and binding maximum (B_{max}).

SDS-PAGE and Far Western Blot of Fg—Human and recombinant Fg proteins were separated on 10% SDS-PAGE using Laemmli sample buffer containing 10 mM dithiothreitol followed by Coomassie Blue staining or electrotransfer to nitrocellulose membrane. Membranes were blocked with Tris-buffered saline with Tween 20 containing 1% BSA followed by probing with Bbp_{N2N3} (15 μg/ml), $ClfA_{N2N3}$ (15 μg/ml), or $SdrG_{N2N3}$ (5 μg/ml). The bound proteins were detected with anti-His monoclonal antibody followed by anti-mouse-AP or rabbit-anti-Bbp_{N2N3}. Membranes were developed using nitro blue tetrazolium/5-bromo-4-chloro-3-indolyl phosphate (Thermo Fisher).

L. lactis-Bbp—The entire *bbp* coding region from strain *S. aureus* B504 (kindly donated by Ed Feil) was ligated into the pKS80 plasmid for constitutive expression (22). The plasmid pKS80-Bbp was transformed into *L. lactis* MG1363 and plated on GM17 supplemented with erythromycin.

S. aureus Newman Expressing Bbp—The *bbp* promoter, coding, and terminator DNA segment from *S. aureus* MRSA252 (kindly provided by the Network on Antimicrobial Resistance in *Staphylococcus aureus* (NARSA)) was subcloned into TOPO-Zero Blunt. Following digestion with BamHI and XbaI, the insert was ligated to the shuttle vector pCU1, and the plasmid pCU1-Bbp was transformed into *E. coli* XL-10 Gold cells (Stratagene). The plasmid was purified and transformed into electrocompetent *S. aureus* RN4220 and plated on brain heart infusion broth with chloramphenicol. Subsequently, pCU1-Bbp was electroporated into electrocompetent Newman DU6023 *clfA5 isdA clfB*::Em^r Δ*sdrCDE*::Tc^r cells (23).

Bacterial Adherence Assays—L. lactis-pKS80-Bbp, *L. lactis*-pKS80, *S. aureus* Newman DU6023-pCU1-Bbp, and Newman DU6023-pCU1 cells were washed and resuspended to A_{600} of 1.0 or 2.0 for *L. lactis* and *S. aureus*, respectively, in PBS supplemented with 0.5 mM magnesium chloride and 0.1 mM calcium chloride Microtiter wells were coated with Fg Aα1–560 or Fg Aα1–575, washed, and blocked with PBS, 1% BSA. Wells were incubated with 0.1 ml of bacterial suspension for 1.5 h at 30 °C for *L. lactis* or 37 °C for *S. aureus* strains. Attached bacteria were detected by crystal violet staining as described previously (23).

Isothermal Titration Calorimetry (ITC)—The interaction between Bbp_{N2N3} protein and soluble Fg Aα peptides (Table 3) was analyzed using a VP-ITC microcalorimeter (MicroCal) at 30 °C in TBS. The cell contained 15 μM Bbp_{N2N3}, and the syringe contained 225 μM. Samples were degassed for 5 min, and titration was performed with a stirring speed of 300 rpm. The initial injection was 5 μl followed by 29 injections of 10 μl at 0.5 μl/s. Data were fitted to a single binding site model and analyzed using Origin version 5 (MicroCal) software.

Multiple Sequence Alignment—Sequences corresponding to the mapped Fg Aα residues from different species were aligned using ClustalW version 2 (24). The sequence gi numbers are as follows: 1304047, canine; 3789958, feline; 296478815, bovine; 1304179, porcine; 33563252, murine; and 11761629, human.

Fibrin Inhibition Assay—Thrombin-catalyzed fibrinogen clotting was studied as described previously (4). Briefly, 150 μl of a 3.0 μM Fg solution was incubated with 10 μl of increasing concentrations (0.3–10 μM) of Bbp_{N2N3}, $SdrG_{N2N3}$, or BSA and 50 μl of thrombin (1.0 NIH unit/ml) in microtiter wells. Clot formation was monitored by measuring the increase in A_{405} and plotted using GraphPad 4.

RESULTS

Bbp_{N2N3} Binds to Human Fibrinogen—The known ligand-binding sites of other MSCRAMMs of the Sdr family have been mapped to the N2N3 domains of the N-terminal A-region of

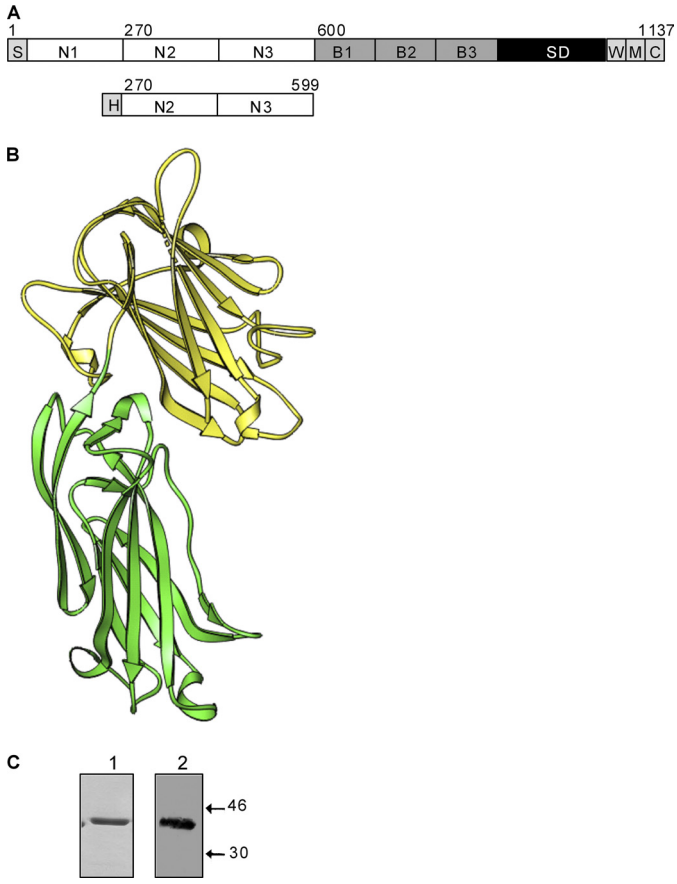

FIGURE 1. **Bbp_{N2N3} construct.** *A*, domain organization of full-length Bbp (*top*) and Bbp_{N2N3} (*bottom*) showing the signal sequence (*S*), amino-terminal subdomains of the A-region (*N1*, *N2*, and *N3*), B-repeats (*B1*, *B2*, and *B3*), serine-aspartate repeat region (*SD*), wall domain (*W*), membrane domain (*M*), carboxyl terminus (*C*), and hexahistidine tag (*H*) in Bbp_{N2N3}. *B*, ribbon representation of the homology model of the N2N3 subdomains of Bbp. The N2 and the N3 subdomains are colored, respectively, in *green* and *yellow*. *C*, purified Bbp_{N2N3} (1 μg/lane) was analyzed by SDS-PAGE Coomassie Blue staining (*lane 1*) or transferred to nitrocellulose for anti-His (*lane 2*) followed by goat-anti-mouse-AP blotting.

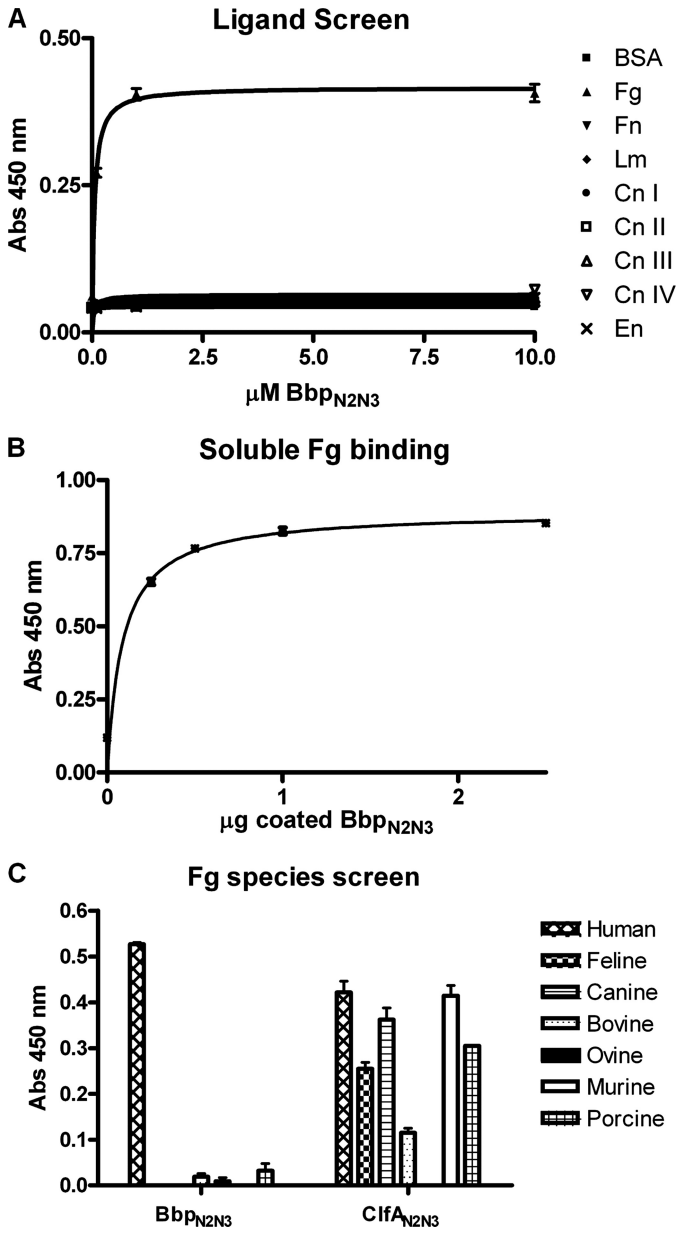

FIGURE 2. **Bbp_{N2N3} binds to fibrinogen.** *A*, a ligand screen was performed on immobilized extracellular matrix and plasma proteins. The putative ligands were immobilized on microtiter wells and probed with increasing concentrations (0.1–10 μM) of Bbp_{N2N3} followed by rabbit-anti-Bbp_{N2N3} and goat-anti-rabbit-HRP. *Abs*, absorbance. *B*, increasing amounts of Bbp_{N2N3} (0.25–2.5 μg) were coated on microtiter wells and probed with 1 μM Fg followed by goat-anti-human Fg and donkey-anti-goat-HRP. *C*, microtiter wells were coated with 1 μg of human, canine, feline, bovine, ovine, murine, or porcine Fg or BSA in bicarbonate buffer overnight. The wells were probed with 500 nM Bbp_{N2N3} or $ClfA_{N2N3}$ followed by protein-specific rabbit polyclonal antibodies and goat-anti-rabbit-HRP. Values represent the mean ± S.E. *Fn*, fibronectin; *Lm*, laminin; *Cn*, collagen; *En*, elastin.

the proteins. We first defined the putative N2N3 domains of Bbp to residues 270–599 (Fig. 1, *A* and *B*) by comparing the sequence of Bbp with that of SdrG and ClfA for which we have previously determined the crystal structures (4, 25, 26). This segment was expressed as a recombinant His-tagged fusion protein and purified using affinity and ion-exchange chromatography (Fig. 1*C*). To explore the ligand binding of Bbp, we conducted an initial screen where increasing concentrations (0.01–10.0 μM) of recombinant His-tagged Bbp_{N2N3} were incubated in microtiter wells coated with a selection of extracellular matrix and plasma proteins (Fig. 2*A*). In this assay, Bbp_{N2N3} bound to Fg in a concentration-dependent, saturable manner but failed to bind to elastin, collagen types I–IV, laminin, fibronectin, and albumin. We also found that soluble Fg bound to increasing amounts of Bbp_{N2N3} coated on microtiter wells (Fig. 2*B*). Thus, the solid-phase assays indicate a specific interaction between Bbp_{N2N3} and Fg regardless of which was immobilized.

We next determined the species specificity of the Fg recognized by Bbp. Human, feline, canine, bovine, ovine, murine, and porcine Fg were used to coat microtiter wells, and the binding of Bbp_{N2N3} to the Fg-coated surfaces was measured. Our results indicate that Bbp_{N2N3} binds only to Fg isolated from human plasma (Fig. 2*C*). These results suggest that Bbp recognizes a specific motif present in human Fg but not found in other Fgs. This restricted specificity is in contrast to that of ClfA, which binds to all of the Fgs tested with the exception of ovine Fg (Fig. 2*C*).

The dissociation constant of the Bbp_{N2N3}-Fg complex was determined using SPR. Binding of increasing concentrations of

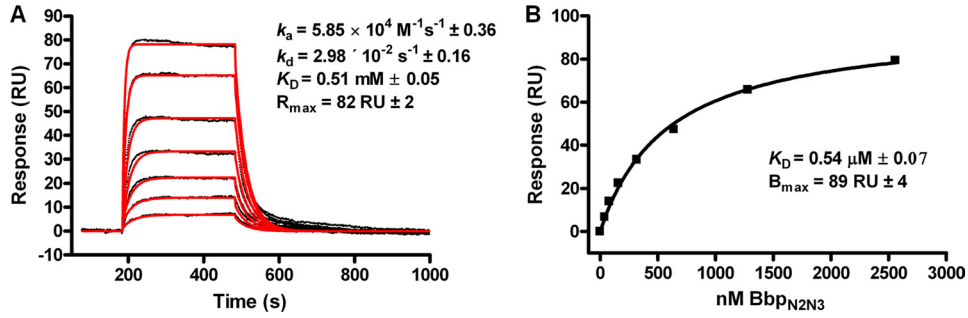

FIGURE 3. **Surface plasmon resonance analysis of Bbp$_{N2N3}$ binding to fibrinogen.** 2-fold linear dilution series (2.56–0.04 μM) of Bbp$_{N2N3}$ were injected over the Fg surface (1600 response units (*RU*)) on a BIAcore sensor chip. *A*, kinetics analysis. Baseline corrected response curves for each injection of Bbp$_{N2N3}$ (shown as *black lines* with lower concentration at the bottom) are overlaid with the global fitting to a 1:1 (Langmuir) binding model (shown in *red*). Kinetic rate constants as well as response maximum (R_{max}) listed in the *inset* were obtained from the fitting. *B*, equilibrium analysis. Responses at equilibrium of the SPR curves were fit to a one-site binding (hyperbola) isotherm (GraphPad Prism 4) to obtain the dissociation equilibrium constant and binding maximum (B_{max}). Data consist of one representative of three experiments. Values represent the mean ± S.E.

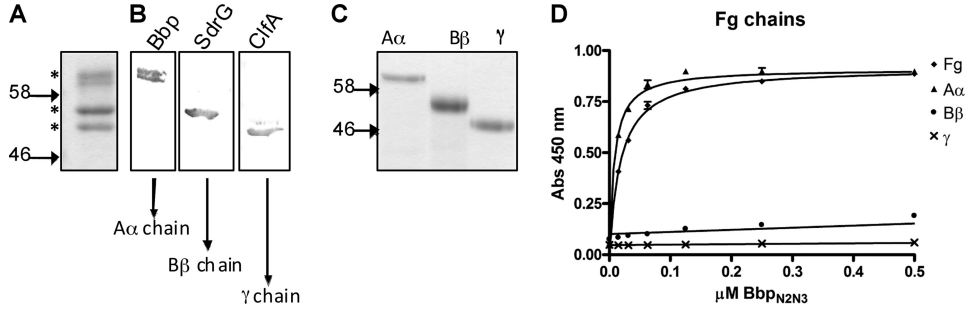

FIGURE 4. **Bbp$_{N2N3}$ recognizes the Aα chain of fibrinogen.** *A* and *B*, Fg was reduced and separated on SDS-PAGE followed by Coomassie Blue staining (*A*) to reveal the three chains (indicated by *asterisks* on *left*) Aα (*top band*), Bβ (*middle band*), and γ (*bottom band*) or electrotransferred for Far Western blotting (*B*). Membranes were probed with Bbp$_{N2N3}$ (*left*), SdrG$_{N2N3}$ (*middle*), and ClfA$_{N2N3}$ (*right*) followed by incubation with protein-specific rabbit polyclonal antibodies and goat-anti-rabbit-AP. *C*, recombinant His-tagged constructs of the individual chains were purified, run on SDS-PAGE, and stained with Coomassie Blue for comparison with reduced human Fg. *D*, Fg and recombinant individual Aα, Bβ, and γ chains were coated on microtiter wells and probed with Bbp$_{N2N3}$ followed by anti-Bbp$_{N2N3}$ and goat-anti-rabbit-HRP. Values represent the mean ± S.E. *Abs*, absorbance.

Bbp$_{N2N3}$ (40 nM-2.56 μM) to Fg immobilized on a sensor chip was analyzed using a BIAcore 3000 (Fig. 3*A*). The results from kinetic and equilibrium analyses revealed K_D values of 510 ± 5 and 540 ± 7 nM, respectively, for the binding of Bbp$_{N2N3}$ to Fg (Fig. 3*B*). The kinetic studies indicate rapid on and off rates ($5.85 \times 10^4\ M^{-1}\ s^{-1} \pm 0.36$ and $2.98 \times 10^{-2}\ s^{-1} \pm 0.16$, respectively), and the equilibrium experiment revealed a binding ratio of 1:1 per dimer of Fg. Together, these data demonstrate that Bbp$_{N2N3}$ binds specifically to human Fg with an affinity similar to that of other Fg-binding MSCRAMMs (3, 11, 14).

Bbp$_{N2N3}$ Recognizes the Aα Chain of Fibrinogen—To locate the Bbp-binding site(s) in Fg, we used Far Western blotting analysis. Fg was reduced in sample buffer containing dithiothreitol to dissociate disulfide bonds, and the three Fg polypeptides were separated by SDS-PAGE (Fig. 4*A*) and transferred to a nitrocellulose membrane. The membrane was probed with different recombinant His-tagged MSCRAMMs, and binding was revealed with an anti-His antibody. In this assay, Bbp$_{N2N3}$ bound to the Aα chain of Fg(Fig. 4*B*), whereas SdrG$_{N2N3}$ and ClfA$_{N2N3}$ bound to their previously reported ligands, the Bβ and γ chains, respectively (4, 14).

To verify our Far Western results, binding of Bbp$_{N2N3}$ to the individual Fg chains was tested. Recombinant full-length Aα, Bβ, and γ chains were expressed as His-tagged constructs and purified (Fig. 4*C*) under denaturing conditions in 8 M urea. Individual chains were coated on microtiter plates, and the binding of increasing concentrations of Bbp$_{N2N3}$ (15.6–500 nM) to the immobilized Fg polypeptides was followed (Fig. 4*D*). Although Bbp$_{N2N3}$ did not recognize the Bβ and γ Fg polypeptides, it bound in a concentration-dependent and saturable manner to plasma Fg and recombinant Fg Aα, indicating that Bbp$_{N2N3}$ binds to a linear sequence in the human Fg Aα chain.

The Binding Site for Bbp Lies within Residues 561–575 of the Fg Aα Chain—To map the Bbp$_{N2N3}$-binding site further, we constructed a series of C-terminal truncates of the Aα chain (Fig. 5*A*). The recombinant Fg Aα1–575 and Fg Aα1–560 were purified (Fig. 5*B*, *lanes 3* and *4*, respectively) and examined for their ability to support Bbp binding. Far Western blots revealed that Aα1–575 retained the Bbp$_{N2N3}$-binding site (Fig. 5*C*, *lane 3*). However, no MSCRAMM binding was detected to Aα1–560 (Fig. 5*C*, *lane 4*), suggesting that Bbp binding to Fg requires a residue(s) in Aα 560–575. To confirm our results, a solid-phase assay comparing the binding of Bbp$_{N2N3}$ to Aα1–560 and Aα1–575 revealed that only Aα1–575 supported a concentration-dependent binding (Fig. 6*A*). These results indicate that residues involved in the binding of Bbp$_{N2N3}$ to Fg lie in the Aα chain between position 561 and 575.

Full-length Bbp Binds to Fg Aα Chain Residues 561–575— The non-pathogenic bacterium *L. lactis* has been successfully used as a heterologous host to display full-length forms of MSCRAMMs on its cell surface (23). This system was used to determine whether Bbp expressed on the surface of a bacterium could recognize the binding domain identified for recombinant Bbp$_{N2N3}$ in Fg Aα. Using a bacterial adherence assay, we deter-

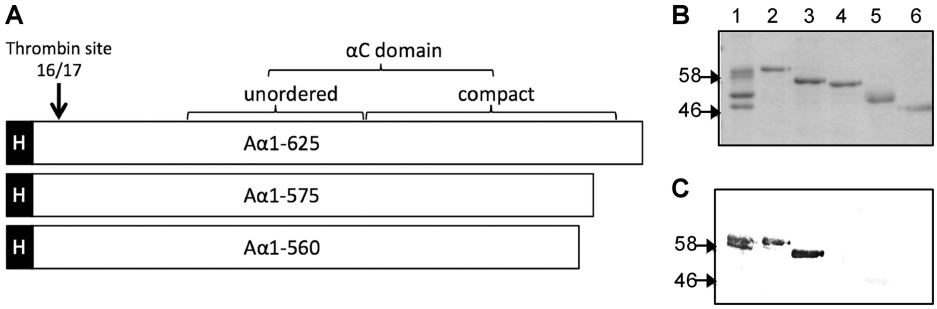

FIGURE 5. **The Bbp_{N2N3}-binding site on Aα lies in residues 561–575.** *A*, schematic of full-length Aα (1–625) and C′-truncated (Aα1–575 and Aα1–560) constructs. *B*, reduced plasma Fg (*lane 1*), purified Aα (*lane 2*), Aα1–575 (*lane 3*), Aα1–560 (*lane 4*), Bβ (*lane 5*), and γ (*lane 6*) chains were separated on SDS-PAGE. *C*, Far western blotting of Fg constructs was performed by incubating the membrane with Bbp_{N2N3} followed by rabbit-anti-Bbp_{N2N3} and goat-anti-rabbit AP.

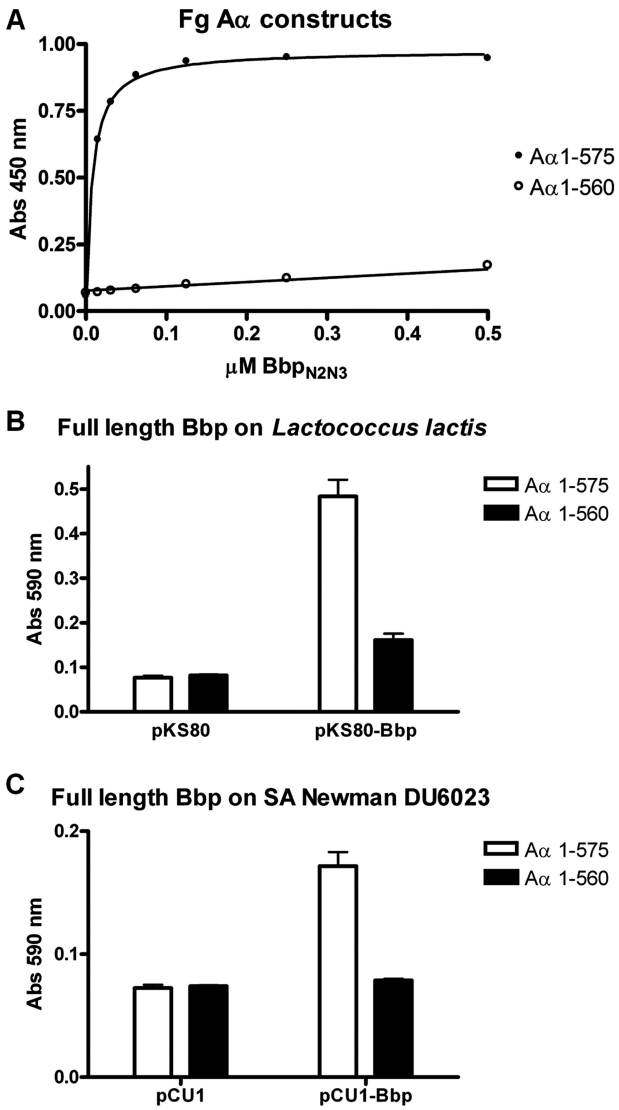

FIGURE 6. **Recombinant Bbp_{N2N3} and full-length Bbp on the surface of cells bind to Fg Aα1–575.** *A*, wells coated with purified Aα1–575 or Aα1–560 were probed with Bbp_{N2N3} followed by rabbit-anti-Bbp_{N2N3} polyclonal antibody and then with goat-anti-rabbit-HRP to detect binding. *Abs*, absorbance. *B* and *C*, adherence of bacteria to Aα1–575 or Aα1–560 was detected with crystal violet staining. *B* and *C*, microtiter wells with coated Aα1–575 or Aα1–560 were incubated with *L. lactis*-pKS80 and *L. lactis*-pKS80-Bbp (*B*) or with *S. aureus* Newman (*SA Newman*) DU6023-pCU1 and *S. aureus* Newman DU6023-pCU1-Bbp (*C*). Values represent the mean ± S.E.

mined that *L. lactis* (pKS80-Bbp) adhered to plates coated with Aα1–575 but not to plates coated with Aα1–560, whereas *L. lactis* carrying the empty pKS80 did not attach to plates coated with either of the Aα truncation mutants (Fig. 6*B*). This result indicates that full-length Bbp expressed on the surface of a bacterium can bind to the identified binding sequence in Fg.

An *S. aureus* Newman mutant that is defective in the MSCRAMMs ClfA, ClfB, IsdA, IsdB, SdrC, SdrD, and SdrE has been constructed (23). This strain was used to express the full-length *bbp* gene under the control of its native promoter. The mutant host carrying the empty vector pCU1 and pCU1-Bbp was tested for adherence to Aα1–575. Newman expressing Bbp attached to wells coated with Aα1–575 but not to immobilized Aα1–560. In contrast, the empty vector control strain did not recognize either Aα construct (Fig. 6*C*). These data indicate that Bbp expressed on the surface of *S. aureus* recognizes the identified binding site and can mediate adherence to human Fg.

Characterization of the Interaction between Bbp and Fg Aα Using Synthetic Peptides—To further define the binding site in Fg Aα for Bbp_{N2N3}, we used synthetic peptides in inhibition experiments. Increasing concentrations (0.1–30 μM) of peptides corresponding to different segments of Fg Aα were preincubated with Bbp_{N2N3} before the mixture was added to Fg-coated wells (Fig. 7*A*). The Aα561–575 peptide fully inhibited the binding of Bbp_{N2N3} to immobilized Fg, whereas a peptide containing the same residues but in a scrambled sequence (AαScr) did not exhibit any inhibitory activity. In a second assay (Fig. 7*B*), 100% inhibition was observed with the peptides Aα551–575, Aα561–575, and Aα556–570. However, the Aα551–565 peptide did not affect the binding of Bbp_{N2N3} to Fg.

The interaction between Bbp_{N2N3} and Fg Aα peptides was further characterized by ITC. Each peptide was tested for binding by titrating a solution of 225 μM peptide into a cell containing 15 μM Bbp_{N2N3} (Fig. 7*C*, *top panels*). The one-binding site fit model was used to analyze the data, which are summarized in Table 4. ITC analysis showed that the peptides Aα551–575 and Aα561–575 bound to Bbp_{N2N3} with K_D values of 796 and 309 nM, respectively, indicating high affinity interactions. Furthermore, no binding to the peptide Aα551–565 was detected, suggesting that these residues are not important for binding. These results are consistent with our data using the truncated Fg Aα chain mutants. The peptide Aα556–570 bound the MSCRAMM with a K_D of 1.8 μM. Therefore, residues contained in this peptide can mediate binding to Bbp_{N2N3}, albeit

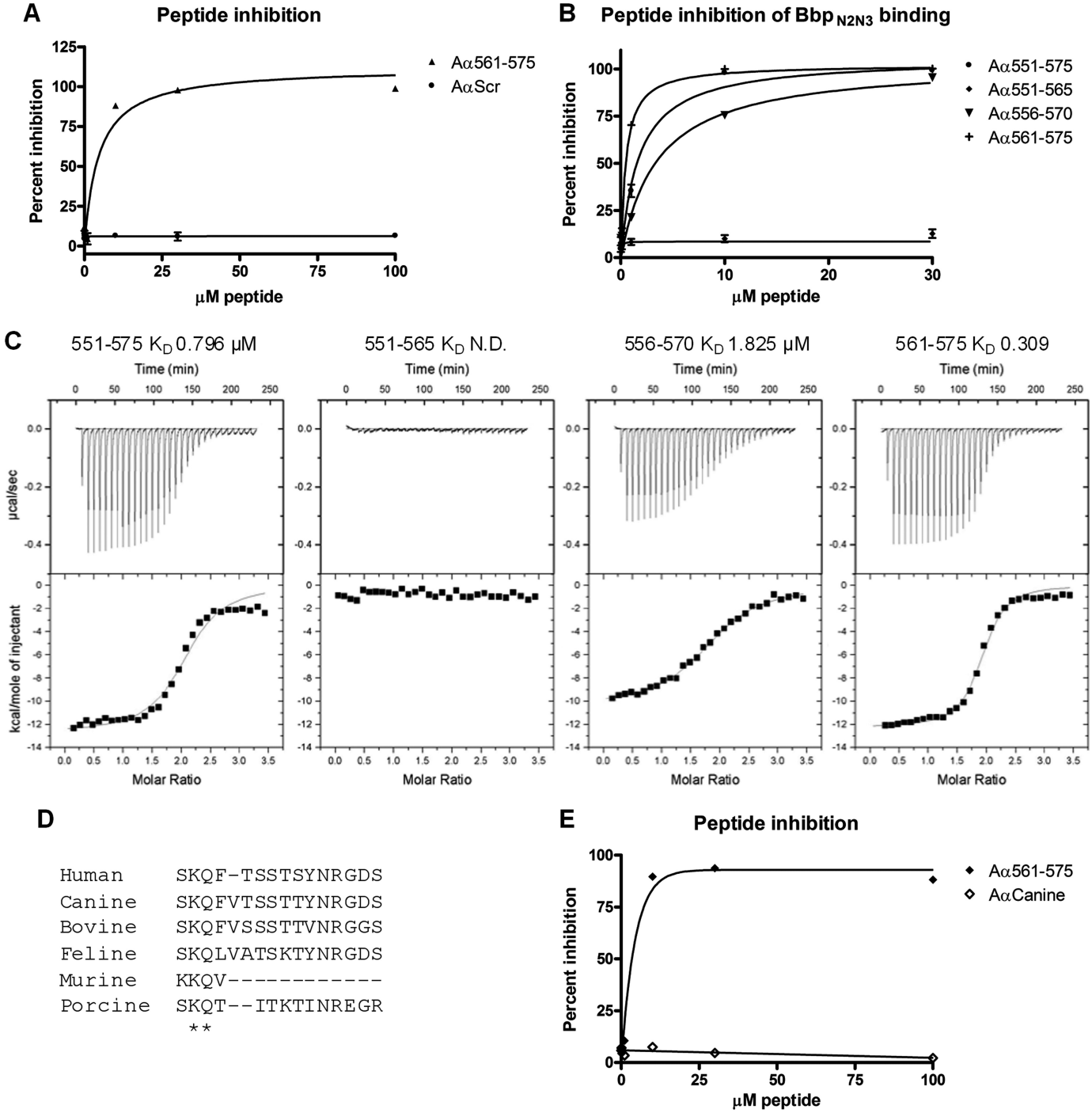

FIGURE 7. **Analysis of the interaction between Bbp_{N2N3} and Fg Aα peptides.** *A*, *B*, and *E*, increasing concentrations of the peptides Aα561–575 and scrambled sequence (*AαScr*) (*A*); Aα551–575, Aα561–575, Aα556–570, and Aα551–565 (*B*); or Aα561–575 and canine Aα (*AαCanine*) (*E*) were preincubated with Bbp_{N2N3} (150 nM) for 30 min before addition to Fg-coated wells in a solid-phase assay to assess inhibition of binding. Values represent the mean ± S.E. *C*, isothermal titration calorimetry of 225 μM Fg Aα peptides and 15 μM Bbp_{N2N3} was measured with a VP-ITC. Thirty titrations of 10 μl of peptides were injected into the cell containing Bbp_{N2N3} (*top panels*). The data were fitted to a one-binding site model (*bottom panels*), and binding affinities are expressed as dissociation constants (K_D) or the reciprocal of the association constants determined by Origin software. *N.D.*, affinity not determined. *D*, ClustalW alignment of the residues corresponding to the human sequence Aα561–575 from different species. *Asterisks* denote conserved residues among all species.

with a lower affinity. The affinities of the peptides for Bbp_{N2N3} correlate nicely with the peptide inhibition data (Fig. 7, *A* and *B*) so that the inhibitory activity exhibited by the peptides directly relates to their ability to bind to Bbp_{N2N3}. Taken together, the truncation analysis experiments, the inhibition data, and the ITC results indicate that Bbp_{N2N3} binds specifically to Aα residues 561–575.

A ClustalW alignment of the Fg Aα 561–575 of Fg from six species was performed (Fig. 7*D*). The results indicate that the sequences of human, canine, and feline fibrinogen are related. All three contain a potential integrin-binding RGD site, whereas only some of the identified binding residues are present in porcine or bovine Fg. Furthermore, the rat and murine sequences are more distant from the human sequence in this

region. Fg from these rodents does not contain the RGD site, nor a stretch of polar, uncharged residues. The alignment data indicate that the feline and canine Fg are the closest to human, with only minor sequence differences, yet neither Fg is recognized by Bbp_{N2N3} (Fig. 2*C*). To further confirm the results obtained with full-length Fg, an inhibition assay was performed with the synthetic peptide corresponding to the Aα 561–575 residues in canine Fg. The Aα canine peptide did not inhibit the ability of Bbp_{N2N3} to bind to Fg (Fig. 7*E*). This result verifies our previous data and confirms that Bbp targets a human-specific sequence in Fg Aα.

Bbp_{N2N3} Inhibits Fibrin Formation—Many MSCRAMMs not only bind to the target molecule in the host but also manipulate the biology of the target. For example SdrG from *S. epidermidis* inhibits coagulation by binding to and covering the thrombin cleavage site in the Fg Bβ-chain. To examine the effect of Bbp on coagulation, Fg was pretreated with increasing concentrations (0.3–10 μM) of Bbp_{N2N3}, $SdrG_{N2N3}$, as a positive control, or BSA as a negative control prior to the addition of thrombin. Bbp_{N2N3} inhibited coagulation in a concentration-dependent manner as effectively as $SdrG_{N2N3}$ (Fig. 8*A*). Human thrombin is capable of cleaving the Fg of other species. Therefore, we examined whether the effect on coagulation exerted by Bbp was species-specific. Bbp_{N2N3} did not inhibit thrombin-catalyzed coagulation of ovine Fg (Fig. 8*B*), which is not recognized by the MSCRAMM. Thus, our results suggest that Bbp can inhibit blood coagulation by binding to Fg.

DISCUSSION

S. aureus appears to use a multitude of virulence factors to cause a wide range of diseases. These virulence factors likely interact with specific molecular targets in the host. Here, we report that Bbp recognizes a specific sequence in the Aα polypeptide of human Fg.

We observed that Bbp_{N2N3} can bind to soluble as well as immobilized native Fg, reduced Fg, and recombinant, denatured Fg Aα chain. These data indicate that the MSCRAMM binds to a linear sequence in the ligand, which is typical of Fg-binding MSCRAMMs. Furthermore, BIAcore experiments with immobilized Fg revealed a K_D of 540 nM for the Bbp_{N2N3} interaction, and a K_D of 309 nM was calculated from ITC experiments where the peptide Aα561–575 was titrated into a solution of Bbp_{N2N3}. The two methods yielded similar K_D values, although in one case, intact immobilized Fg was the binding partner, and in the other, a soluble linear Fg peptide was used. This suggests that the peptide sequence contains all Bbp-interacting residues in Fg. Furthermore, the K_D determined for the Bbp/Fg peptide interaction is similar to those determined for the binding of Fg peptides to the staphylococcal MSCRAMMs SdrG (380 nM), ClfA (5.8 μM), and FnbpA (2.4 μM), although Bbp binds to a site distinctly different from those recognized by the other Fg-binding MSCRAMMs (3, 11, 27).

Bbp_{N2N3} only targets human Fg, demonstrating a high degree of specificity of the interaction. Alignment of the sequences corresponding to the human Fg Aα561–575 in Fg from other species revealed small differences among the residues present in human, feline, and canine Fg. Specifically, the canine sequence contains an extra hydrophobic residue at (human) position 565. This offsets the stretch of polar, uncharged residues found between 565 and 571 by one position. Also, Ser^{569} in human is a Thr in the canine sequence. These are the only two differences between the human and canine sequences, but apparently, they are sufficient to abrogate Bbp_{N2N3} binding to canine Fg as the Aα canine peptide had no effect on Bbp_{N2N3} binding to Fg. The structural basis for this remarkable restricted ligand specificity is currently under investigation.

The ability of Bbp to bind Fg was initially demonstrated with recombinant Bbp_{N2N3} and was confirmed using constructs that express the full-length protein on the surface of two bacterial hosts. *L. lactis* and an *S. aureus* Newman mutant devoid of all known fibrinogen-binding MSCRAMMs provided a platform to study the ability of the single MSCRAMM to engage in ligand binding (23). In this study, Bbp on the surface of both bacteria mediated attachment to immobilized Aα1–575 but not to Aα1–560 (Fig. 6, *B* and *C*). These data indicate that the full-length Bbp protein expressed on the surface of a bacterium can mediate attachment to a Fg substrate.

The binding site for Bbp_{N2N3} was mapped to Aα561–575 in the Fg molecule, which ends with the second RGDS site of the Aα chain. Reports have suggested a role for the second Aα RGD site in binding to the integrins $\alpha_5\beta_1$ and $\alpha_V\beta_3$ (28). Although further studies are required to determine what downstream effects Bbp binding could have on Fg biology, one possible effect could be a modulation of the Fg Aα-integrin interaction.

TABLE 4
Isothermal titration calorimetry data
ND, not determined.

	N	*K*	Δ*H*	Δ*S*	*K* (calculated)
			kcal/mol	*kcal/mol*	
551–575	2.074	1.26×10^6	-1.27×10^4	−13.95	0.796 μM
551–565	ND	ND	ND	ND	ND
556–570	1.894	5.48×10^5	-1.04×10^4	−8.03	1.825 μM
561–575	1.902	3.23×10^6	-1.22×10^4	−10.51	0.309 μM

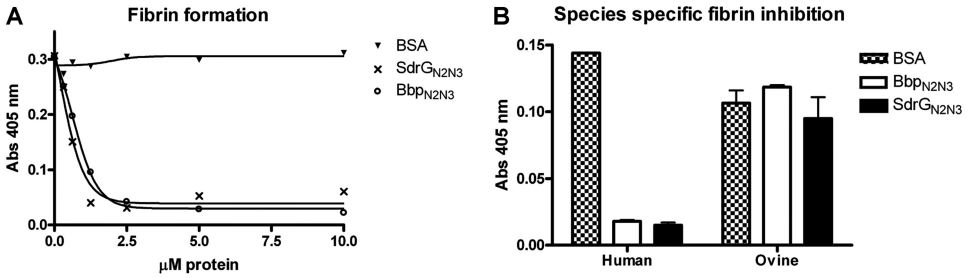

FIGURE 8. **Bbp_{N2N3} inhibits fibrin formation.** *A* and *B*, increasing concentrations (0.3–10 μM) (*A*) or 1 μM (*B*) of BSA, $SdrG_{N2N3}$, or Bbp_{N2N3} were preincubated with human Fg-coated (*A* and *B*) or ovine Fg-coated (*B*) wells prior to the addition of α-thrombin. Values represent the mean ± S.E. *Abs*, absorbance.

Experiments demonstrate that Bbp can inhibit thrombin-induced blood coagulation. The effect is of a similar potency as that previously observed for SdrG. However, whereas SdrG binding to Fg interferes with thrombin-induced release of the fibrinopeptide B, the mechanism of the anticoagulant action of Bbp is presently unclear.

Bone sialoprotein was previously described as a ligand of Bbp (29). This interaction may play a specific role in the pathogenesis of osteomyelitis, an infection of the bone, which may be caused by hematogenous spread. Therefore, it is possible that Bbp may function in two capacities: (i) as an important factor in the colonization of bone tissue and (ii) as a contributing factor in *S. aureus* hematologic diseases, such as sepsis. Future studies regarding the expression profile of Bbp in different disease settings or the role of the MSCRAMM in disease-specific models may aid in elucidating the contribution of Bbp to *S. aureus* pathogenesis.

Acknowledgments—We acknowledge NARSA for providing S. aureus MRSA252. Drs. Ed Feil, University of Bath, and Ross Fitzgerald, University of Edinburgh, are acknowledged for helpful discussion.

REFERENCES

1. Lowy, F. D. (1998) *N. Engl. J. Med.* **339,** 520–532
2. Foster, T. J., and Höök, M. (1998) *Trends Microbiol.* **6,** 484–488
3. Ponnuraj, K., Bowden, M. G., Davis, S., Gurusiddappa, S., Moore, D., Choe, D., Xu, Y., Hook, M., and Narayana, S. V. L. (2003) *Cell* **115,** 217–228
4. Davis, S. L., Gurusiddappa, S., McCrea, K. W., Perkins, S., and Höök, M. (2001) *J. Biol. Chem.* **276,** 27799–27805
5. Bowden, M. G., Heuck, A. P., Ponnuraj, K., Kolosova, E., Choe, D., Gurusiddappa, S., Narayana, S. V., Johnson, A. E., and Höök, M. (2008) *J. Biol. Chem.* **283,** 638–647
6. Kollman, J. M., Pandi, L., Sawaya, M. R., Riley, M., and Doolittle, R. F. (2009) *Biochemistry* **48,** 3877–3886
7. Mosesson, M. W., Siebenlist, K. R., and Meh, D. A. (2001) *Ann. N.Y. Acad. Sci.* **936,** 11–30
8. Gailit, J., Clarke, C., Newman, D., Tonnesen, M. G., Mosesson, M. W., and Clark, R. A. (1997) *Exp. Cell Res.* **232,** 118–126
9. McDevitt, D., Francois, P., Vaudaux, P., and Foster, T. J. (1994) *Mol. Microbiol.* **11,** 237–248
10. Ní Eidhin, D., Perkins, S., Francois, P., Vaudaux, P., Höök, M., and Foster, T. J. (1998) *Mol. Microbiol.* **30,** 245–257
11. Wann, E. R., Gurusiddappa, S., and Hook, M. (2000) *J. Biol. Chem.* **275,** 13863–13871
12. Rivera, J., Vannakambadi, G., Höök, M., and Speziale, P. (2007) *Thromb. Haemost.* **98,** 503–511
13. Walsh, E. J., Miajlovic, H., Gorkun, O. V., and Foster, T. J. (2008) *Microbiology* **154,** 550–558
14. McDevitt, D., Nanavaty, T., House-Pompeo, K., Bell, E., Turner, N., McIntire, L., Foster, T., and Höök, M. (1997) *Eur. J. Biochem.* **247,** 416–424
15. Hair, P. S., Ward, M. D., Semmes, O. J., Foster, T. J., and Cunnion, K. M. (2008) *J. Infect. Dis.* **198,** 125–133
16. Walsh, E. J., O'Brien, L. M., Liang, X., Hook, M., and Foster, T. J. (2004) *J. Biol. Chem.* **279,** 50691–50699
17. Holden, M. T., Feil, E. J., Lindsay, J. A., Peacock, S. J., Day, N. P., Enright, M. C., Foster, T. J., Moore, C. E., Hurst, L., Atkin, R., Barron, A., Bason, N., Bentley, S. D., Chillingworth, C., Chillingworth, T., Churcher, C., Clark, L., Corton, C., Cronin, A., Doggett, J., Dowd, L., Feltwell, T., Hance, Z., Harris, B., Hauser, H., Holroyd, S., Jagels, K., James, K. D., Lennard, N., Line, A., Mayes, R., Moule, S., Mungall, K., Ormond, D., Quail, M. A., Rabbinowitsch, E., Rutherford, K., Sanders, M., Sharp, S., Simmonds, M., Stevens, K., Whitehead, S., Barrell, B. G., Spratt, B. G., and Parkhill, J. (2004) *Proc. Natl. Acad. Sci. U.S.A.* **101,** 9786–9791
18. Lord, S. T. (1985) *DNA* **4,** 33–38
19. Bolyard, M. G., and Lord, S. T. (1989) *Blood* **73,** 1202–1206
20. Bolyard, M. G., and Lord, S. T. (1988) *Gene* **66,** 183–192
21. Carson, M. (1997) *Methods Enzymol.* **277,** 493–505
22. Hartford, O., O'Brien, L., Schofield, K., Wells, J., and Foster, T. J. (2001) *Microbiology* **147,** 2545–2552
23. Corrigan, R. M., Miajlovic, H., and Foster, T. J. (2009) *BMC Microbiology* **9,** 22
24. Larkin, M. A., Blackshields, G., Brown, N. P., Chenna, R., McGettigan, P. A., McWilliam, H., Valentin, F., Wallace, I. M., Wilm, A., Lopez, R., Thompson, J. D., Gibson, T. J., and Higgins, D. G. (2007) *Bioinformatics* **23,** 2947–2948
25. Josefsson, E., McCrea, K. W., Ní Eidhin, D., O'Connell, D., Cox, J., Höök, M., and Foster, T. J. (1998) *Microbiology* **144,** 3387–3395
26. Deivanayagam, C. C., Perkins, S., Danthuluri, S., Owens, R. T., Bice, T., Nanavathy, T., Foster, T. J., Höök, M., and Narayana, S. V. (1999) *Acta Crystallogr D Biol. Crystallogr.* **55,** 554–556
27. Ganesh, V. K., Rivera, J. J., Smeds, E., Ko, Y. P., Bowden, M. G., Wann, E. R., Gurusiddappa, S., Fitzgerald, J. R., and Höök, M. (2008) *PLoS Pathog.* **4,** e1000226
28. Suehiro, K., Mizuguchi, J., Nishiyama, K., Iwanaga, S., Farrell, D. H., and Ohtaki, S. (2000) *J. Biochem.* **128,** 705–710
29. Tung, H., Guss, B., Hellman, U., Persson, L., Rubin, K., and Rydén, C. (2000) *Biochem. J.* **345,** 611–619

Fibrinogen Is a Ligand for the *Staphylococcus aureus* Microbial Surface Components Recognizing Adhesive Matrix Molecules (MSCRAMM) Bone Sialoprotein-binding Protein (Bbp)

Vanessa Vazquez, Xiaowen Liang, Jenny K. Horndahl, Vannakambadi K. Ganesh, Emanuel Smeds, Timothy J. Foster and Magnus Hook

J. Biol. Chem. 2011, 286:29797-29805.
doi: 10.1074/jbc.M110.214981 originally published online June 3, 2011
